MUON ARRIVAL TIME DISTRIBUTIONS OF SIMULATED EXTENSIVE AIR SHOWERS IN VIEW OF MASS DISCRIMINATION*

I.M. Brancus[a], H. Rebel[b], M. Duma[a], A.F. Badea[a,b]
C. Aiftimiei[a] and J. Oehlschlaeger[b]

[a]IFIN-HH Bucharest, P.O. Box MG-6, 76900, Romania
[b] Forschungszentrum Karlsruhe, Postfach 3640, 76021 Karlsruhe, Germany

(Received December 4, 2001)

By extensive Monte Carlo simulations of Extensive Air Showers (EAS), using the EAS simulation code CORSIKA, arrival time distributions of the EAS muon have been generated for iron, oxygen and proton induced air showers using different hadronic interaction models as Monte Carlo generators. The muon time profiles up to distances of 310 m from the core position have been obtained for different primaries. Applying non-parametric statistical inference methods it is shown that a reliable determination of the shower age, correlated with the time parameters would lead to a relatively good discrimination of showers of different primary mass.

PACS numbers: 96.40.Pq

1. Introduction

The temporal structure of the muon component of EAS is of great interest for detailed understanding of the EAS structure, since it reflects the longitudinal EAS development [1-3]. Introducing the travel distance l_μ of the muon from the height of production by the hadronic collisions, a simple triangulation procedure (Fig. 1) displays the relation between the height of production of the muon and its time-of-flight or its angle-of-incidence.

Thus, for two muons produced at different heights and registered at the same distance from the shower core, a smaller travel time results for the higher height as muons produced by iron, with a small interaction length in the atmosphere. In the case of two muons produced at the same height, the muon detected at larger distance have a longer travel time.

* Presented at the XXVII Mazurian Lakes School of Physics, Krzyże, Poland, September 2–9, 2001.

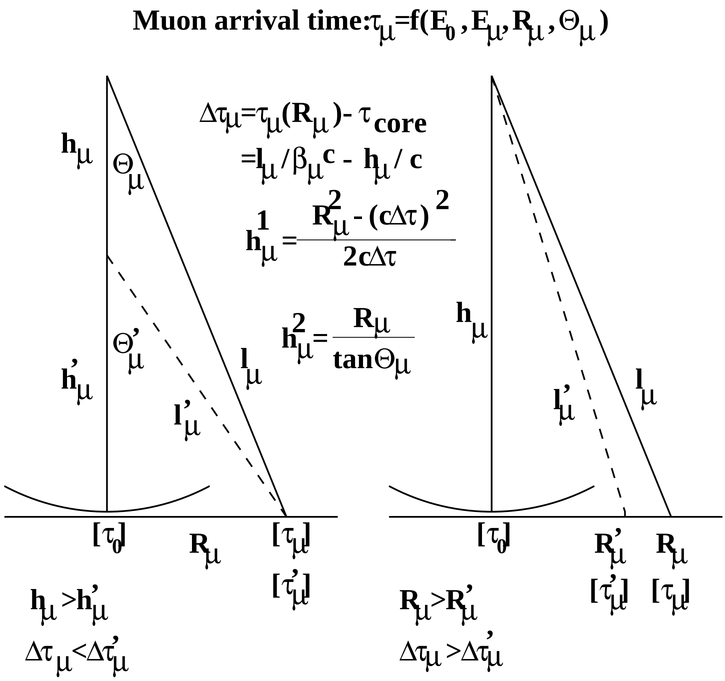

Fig. 1. Geometric description of muon travel from its production from the decay of a hadron to the detection place R_μ.

The relative muon arrival times τ_μ^1, $\tau_\mu^2, \ldots$ at a radial distance R_μ refer to a defined zero-time, usually the arrival time τ_0 of the shower core, called "global quantities"

$$\varDelta\tau_\mu^{n\,\mathrm{glob}} = \tau_\mu^n(R_\mu) - \tau_c\,.$$

When the arrival time τ_c is difficult to determine with sufficient experimental precision, "local" times are considered, which refer to the foremost muon $\tau_\mu^1(R_\mu)$, locally registered by the detector

$$\varDelta\tau_\mu^{n\,\mathrm{loc}} = \tau_\mu^n(R_\mu) - \tau_\mu^1(R_\mu)\,,$$

(with omitting further the label "loc").

The single relative arrival time distributions can be characterised by the mean values $\varDelta\tau_{\mathrm{mean}}$, and by the quartiles $\varDelta\tau_q$, like the median $\varDelta\tau_{0.50}$, the first quartile $\varDelta\tau_{0.25}$ and the third quartile $\varDelta\tau_{0.75}$ [4]. Measurements of muon arrival time distributions are a subject of the current investigations of the KASCADE experiment [4,5]. Using advanced statistical techniques [7], the analysis performed in this paper is based on previous studies [6] of simulated showers for ideal cases, neglecting influences of the detection system.

2. Time profiles of the EAS muon component

The EAS development has been simulated by the Monte Carlo program CORSIKA [8], invoking different models for the hadronic interaction: QGSJET [9], VENUS [10] and SIBYLL [11] for 500 proton and iron induced EAS of the primary energy of 10^{15} eV.

Fig. 2 shows the median arrival time distributions for proton and iron initiated showers at different distances from the shower cores, the radial dependence of their mean values the muon shower profile.

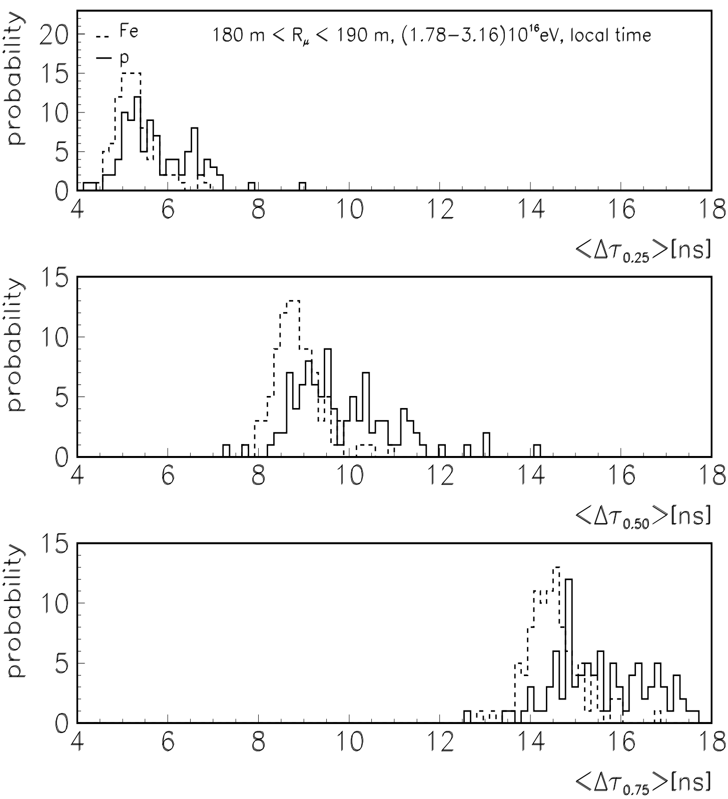

Fig. 2. Distributions of muon arrival times, $\Delta\tau_{0.25}$, $\Delta\tau_{0.50}$ and $\Delta\tau_{0.75}$, originating from p and Fe induced showers.

Fig. 3 displays time profiles for $\Delta\tau_{0.50}$ and $\Delta\tau_{0.50}/\rho_\mu(R_\mu)$ distributions for two different primaries (p, Fe) of the energy 10^{15} eV and comparing three different hadronic interaction models. Using the $\Delta\tau_{0.50}/\rho_\mu(R_\mu)$ results in an improvement of the mass discrimination, especially of the discrimination of different models. This effect is due to the lateral muon density distribution.

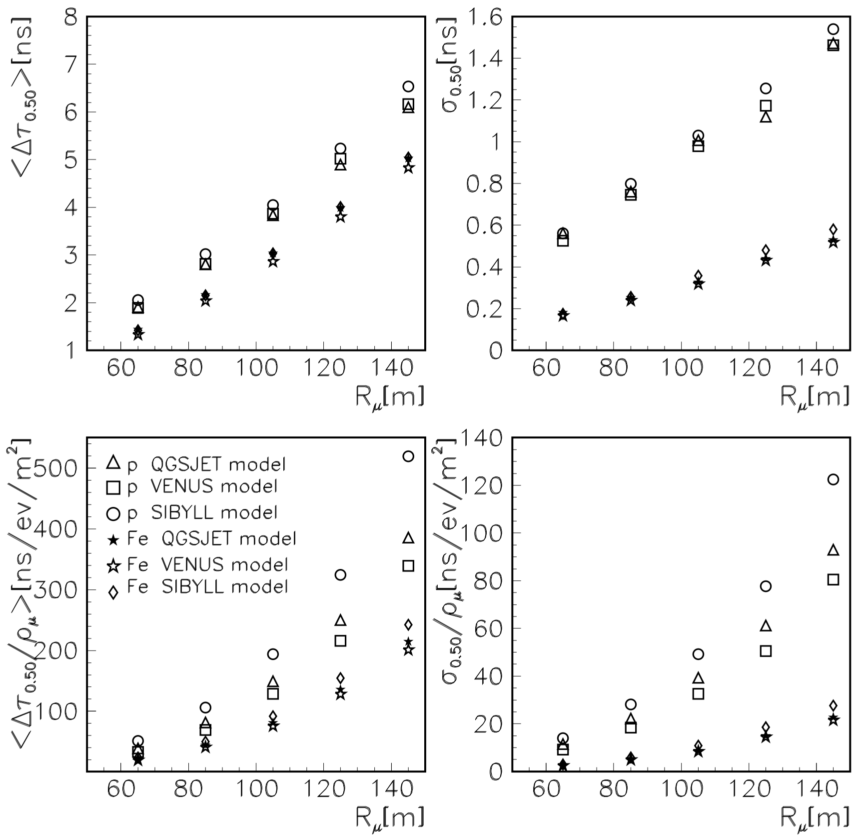

Fig. 3. Simulated muon profiles for $\Delta\tau_{0.50}$ and $\Delta\tau_{0.50}/\rho_\mu$ distributions and their standard deviations of the median values for two primaries p and Fe.

3. Correlated distributions

Special interest is focused to the correlation with the so-called shower age, which indicates the status of the EAS development. The use of NKG approximation [12] does not describe the realistic situation of the electromagnetic component development, so that full Monte Carlo simulations of the electromagnetic component (using the option EGS in the CORSIKA code) have been also performed [13]. 250 EAS have been simulated, initiated by proton and iron primaries with two different incident energies 10^{15} eV and 10^{16} eV, respectively, using two hadronic interaction models: QGSJET and VENUS and applying the NKG-approximation and the full Monte Carlo (EGS) simulations.

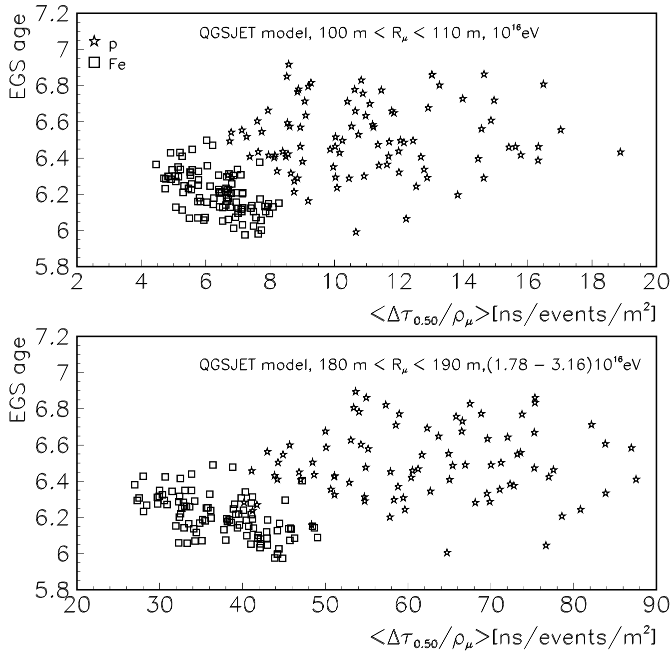

Fig. 4. Correlation of $\Delta\tau_{0.50}/\rho_\mu$ for proton and iron induced EAS with the shower age calculated in EGS approximations for two radial distances: $100\,\mathrm{m} < R_\mu < 110\,\mathrm{m}$ and $180\ \mathrm{m} < R_\mu < 190$ m.

Fig. 4 compares the correlation of the age with $\langle \Delta\tau_{0.50}(R_\mu)/\rho_\mu(R_\mu)\rangle$ at two different distances R_μ from the shower core, for p and Fe showers with energies in the range (1.78–3.16) $\times 10^{16}$ eV. An improvement of the mass discrimination is observed at larger distances from the shower centre.

4. Non-parametric statistical analysis

Non-parametric statistical methods enable the study of multidimensional observable-distributions associating the single observed events to different classes (in our case to p, O and Fe primaries) by comparing the observed events with the model distributions based on Bayesian decision [7]. For each class of primaries 200 showers with energies in the range (1.0–1.78)$\times 10^{15}$ eV, 100 showers with energies in the range (1.0–1.78)$\times 10^{16}$ eV and 50 showers with energies in the range (1.78–3.16)$\times 10^{16}$ eV of vertical incidence have been generated for QGSJET and VENUS models, and the multidimensional distributions of various EAS observables have been analysed.

Results about the classification and misclassification probabilities are given in Table I and Fig. 5 and show an improved mass discrimination at higher energies, in particular when correlated with the shower age.

TABLE I

The classification and misclassification probabilities by correlating age — $\Delta\tau_{0.50}/\rho_\mu$ at $90\,\mathrm{m} \leq R_\mu < 100\,m$ for different energies **1**: $(1.0 - 1.78)\ \times 10^{15}$ eV; **2**: $(1.0 - 1.78)\ \times 10^{16}$ eV; **3**: $(1.78 - 3.16)\times 10^{16}$ eV

Mode	P ↓			O ↓			Fe ↓			error
	P	O	Fe	P	O	Fe	P	O	Fe	
1	0.70	0.28	0.01	0.14	0.56	0.30	0.00	0.19	0.81	0.31
2	0.73	0.25	0.02	0.09	0.71	0.20	0.00	0.21	0.79	0.26
3	0.73	0.24	0.03	0.06	0.72	0.22	0.00	0.07	0.93	0.21

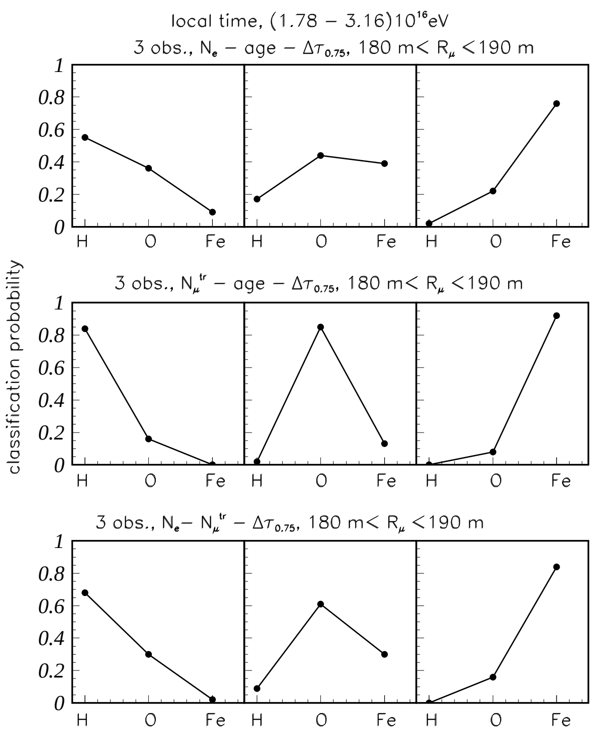

Fig. 5. The classification and misclassification probabilities from muon arrival time distributions correlated with shower age, N_e and N_μ^{tr}.

5. Conclusions

Advanced non-parametrical statistical methods based on Bayesian decision rules have been applied in view of features discriminating the mass of the cosmic primary and different hadronic interaction models. The correlations of the local muon arrival time variables with the local muon density improves the true classification rate and discrimination features. The classification gets improved for higher incident energies and by the correlation with the shower age, and with the shower size N_e and N_μ^{tr}. Correlating the observation of $\Delta\tau_q/\rho_\mu$ for larger radial distances, the mass discrimination of the primaries is slightly improved. Comparing the classification rates for different muon arrival time quantities, both considered models QGSJET and VENUS lead to similar corresponding results. The presented results predicts an enhancement of the discriminative features by the extension of KASCADE detector array to a larger area in KASCADE GRANDE experiment [14].

REFERENCES

[1] J. Linsley *et al.*, *Phys. Rev.* **92**, 485 (1961).

[2] T.V. Danilova *et al.*, *J. Phys. G* **20**, 961 (1995).

[3] H. Rebel *et al.*, *J. Phys. G* **21**, 451 (1995).

[4] I.M. Brancus *et al.*, Proc. ICRC, Salt Lake City, USA, Aug. 1999, eds. D. Kieda *et al.*, vol. 1, 1999, p. 345.

[5] T. Antoni *et al.*, *Astr. Part. Phys.* **15**, 149 (2001).

[6] I.M. Brancus, Internal Report KASCADE-09/2000-02.

[7] A.A. Chilingarian, *Comput. Phys. Commun.* **54**, 381 (1989); A.A. Chilingarian, ANI Reference Manual, 1999.

[8] D. Heck *et al.*, FZKA-Report, p. 6019, Forschungszentrum, Karlsruhe 1998.

[9] N.N. Kalmykov *et al.*, *Nucl. Phys. B. Proc. Suppl.* **52**, 17 (1997).

[10] K. Werner, *Phys. Rep.* **232**, 87 (1993).

[11] R.S. Fletcher *et al.*, *Phys. Rev.* **D50**, 5710 (1994).

[12] K. Greisen, *Ann. Rev. Nucl. Sci.* **10**, 63 (1960).

[13] T. Antoni *et al.*, *Astr. Part. Phys.* **14**, 245 (2001).

[14] M. Bertaina *et al.*, Proc. 27th ICRC Hamburg, Germany, 2001, p. 792.